

# CircPRKCI regulates proliferation, migration and cycle of lung adenocarcinoma cells by targeting miR-219a-5p-regulated CAMK1D

M.-H. SUI, W.-W. ZHANG, D.-M. GENG, D.-J. SUN

Department of Medical Oncology, The Affiliated Yantai Yuhuangding Hospital of Qingdao University, Yantai, China

**Abstract.** – **OBJECTIVE:** Circular ribonucleic acids (circRNAs) are considered as the key regulatory factors for human malignancies in recent years, and lung adenocarcinoma (LUAD) is a common malignancy worldwide, but the molecular mechanism of circRNAs in LUAD has not been completely investigated. Therefore, the mechanism by which circRNA protein kinase C iota (circPRKCI) regulates LUAD cell migration proliferation, and cycle was preliminarily explored in this research, so as to provide new ideas for the treatment of LUAD.

**PATIENTS AND METHODS:** First of all, the circPRKCI expression level in LUAD tissues was tested via quantitative reverse transcription-polymerase chain reaction (qRT-PCR) assay, and the relationship between circPRKCI and the patients' prognosis was analyzed. Then, circPRKCI expression was inhibited by small interfering RNA (siRNA), and the influence of circPRKCI on LUAD cells' ability to proliferate was verified via 5-ethynyl-2'-deoxyuridine (EdU) and cell counting kit-8 (CCK-8) assays. Moreover, the influence of circPRKCI on LUAD cells' ability to migrate was testified by transwell assay, and the regulation of LUAD cell cycle by circPRKCI was confirmed by flow cytometry. The micro RNAs (miRNAs) with binding sites to the 3' untranslated region (UTR) of circPRKCI and the genes binding to miRNAs were discovered using bioinformatics websites, and their associative relation was further explored through Dual-Luciferase reporter gene assay, qRT-PCR assay, Pearson correlation analysis and reverse experiment.

**RESULTS:** It was verified via qRT-PCR assay that circPRKCI was expressed at a remarkably higher level in LUAD tissues relative to that in paracancerous normal tissues. The highly expressed circPRKCI led to poor prognosis of patients. Besides, qRT-PCR assessment results indicated that circPRKCI expression level rose notably in LUAD cell lines, while it was lowered markedly in LUAD cells transfected with si-circPRKCI. According to CCK-8 and EdU as-

say results, the proliferative ability of LUAD cells was weakened clearly after knocking down circPRKCI. It was manifested in the results of transwell assay that the knockdown of circPRKCI significantly repressed the capacity of LUAD cells to migrate. Furthermore, the results of cell cycle test displayed that inhibiting circPRKCI could induce the arrest of LUAD cell cycle in the G1 phase. It was discovered through bioinformatics websites that miR-219a-5p had binding sites to circPRKCI 3'UTR, and the results of Dual-Luciferase reporter gene assay revealed that circPRKCI was able to bind to miR-219a-5p. It was uncovered by the qRT-PCR assay results that miR-219a-5p was lowly expressed in LUAD tissues, and its relative expression had an inverse relation with that of circPRKCI according to the Pearson correlation analysis. In addition, it was shown in the results of reverse experiment that miR-219a-5p could regulate the influence of circPRKCI on the malignant phenotype of LUAD. It was found by means of bioinformatics websites that calcium/calmodulin dependent protein kinase ID (CAMK1D) was a downstream target gene of miR-219a-5p and could be the two conjugated with each other based on the results of Dual-Luciferase reporter gene assay. Moreover, qRT-PCR assay findings illustrated that CAMK1D was evidently highly expressed in LUAD tissues, and the results of Pearson correlation analysis revealed that CAMK1D expression exhibited a negative association with that of miR-219a-5p and a positive correlation with that of circPRKCI.

**CONCLUSIONS:** CircPRKCI is significantly highly expressed in LUAD, and the highly expressed circPRKCI is capable of facilitating LUAD cell migration, proliferation and cycle. CircPRKCI may regulate the malignant phenotype of LUAD via the miR-219a-5p/CAMK1D axis.

*Key Words:*

Lung adenocarcinoma, CircPRKCI, MiR-219a-5p, Cell proliferation, Cell migration.

## Introduction

Around the world, non-small cell lung cancer (NSCLC) is a common malignancy, taking up about 80% of total cases of lung cancer<sup>1</sup>. It is estimated that around 1 million new lung cancer cases occur every year around the world<sup>2</sup>. As the most prevalent type of lung cancer, lung adenocarcinoma (LUAD) takes a proportion of 30-35% in primary lung cancers, which can be treated by surgery, chemotherapy, radiotherapy and molecular targeted therapy, but a substantial proportion of patients will ultimately die of the disease<sup>3</sup>. In spite of recent great improvements in the treatment methods for LUAD, the overall five-year survival rate of NSCLC patients is less than 20%<sup>4</sup>. Hence, it is particularly essential to investigate the molecular mechanism of LUAD to provide novel targets for treating the disease.

Circular ribonucleic acids (circRNAs) are a category of new RNAs formed by covalently closed loops, with neither 5'- and 3'-ends nor polyadenylic acid tails<sup>5</sup>. They are highly stable due to their covalently closed loop structure rather than linear structure<sup>6</sup>. As high-throughput sequencing technique and bioinformatics progress, the detection of circRNAs becomes more and more convenient<sup>7</sup>. CircRNAs are regarded as sponges of micro RNAs (miRNAs), which can regulate RNA-binding proteins and control such tumor cell biological processes as migration, apoptosis and proliferation<sup>8</sup>. There are a growing number of studies on circRNAs in human malignant tumors in recent years. So, hsa\_circRNA\_103809 modulates colorectal cancer cells to migrate and proliferate through the miR-532-3p/FOXO4 axis<sup>9</sup>. CircRNA\_100290 exerts its effect as a sponge of the miR-29 family, so as to play an oncogene role in oral cancer<sup>10</sup>. Moreover, circ\_100395 represses the progression of lung cancer by modulating the miR-1228/TCF21 pathway<sup>11</sup>. However, the role of circRNA protein kinase C iota (circPRKCI) in LUAD has not been thoroughly studied, which needs to be further explored.

MiRNAs, 20-23-nt long, are endogenous, single-stranded, non-coding RNAs<sup>12</sup>, are implicated in modulating genes at the post-transcriptional level through partially complementary binding to the 3' untranslated regions (UTRs) of target mRNAs<sup>13</sup>. Abnormally expressed miRNAs exert pivotal effects in diverse physiopathological processes in human, including cell differentiation, proliferation and tumorigenesis<sup>14</sup>. Increasingly more studies have been conducted for miRNAs

in human malignancies for the past few years. It has been observed that, miR-155 promotes the proliferation of glioma cells by binding to CDX1 in a targeted manner<sup>15</sup>. MiR-214 stimulates nasopharyngeal carcinoma cells to proliferate and inhibits their apoptosis through targeted binding to Bax<sup>16</sup>. Besides, miR-519c-3p facilitates the growth and metastasis of hepatocellular carcinoma *via* targeting BTG3<sup>17</sup>. MiRNAs exert crucial effects in human malignancies, but the function of miR-219a-5p in LUAD has not been completely researched, and further investigations are needed.

Qiu et al<sup>18</sup> revealed that circPRKCI is aberrantly highly expressed in LUAD, but the specific mechanism of action remains unclear. From this perspective, a series of *in vitro* experiments were adopted in this research to investigate the mechanism of circPRKCI in the onset and progression of LUAD, thereby offering new targets for treating the disease.

## Patients and Methods

### Sample Collection

In this research, a total of 50 pairs of tumor tissue samples and paracancerous normal tissue samples were harvested from LUAD patients undergoing no chemotherapy or radiotherapy before surgery. All the surgically resected tissues were quickly preserved in liquid nitrogen at -80°C. The pathological type and stage of tumor were determined as per the UICC staging criteria. All participants were not treated with radiotherapy and chemotherapy before operation. The gastric tumor tissues were confirmed by two pathologists in our hospital. Other kind of tumor that migrated to the stomach was excluded. The informed consent was obtained from all the participants in this research, and this research obtained the approval of the Ethics Committee of The Affiliated Yantai Yuhuangding Hospital of Qingdao University.

### Cell Culture

H1975, A549, H1299 and HBE (a normal human bronchial epithelial cell line) Calu-3 (LUAD cell lines) bought from the Chinese Academy of Sciences (Beijing, China) were cultured with RPMI-1640 medium provided by Invitrogen (Carlsbad, CA, USA) containing 10% fetal bovine serum (FBS) (Invitrogen, Carlsbad, CA, USA) and 1% penicillin/streptomycin from Sigma-Aldrich (St. Louis, MO, USA) in a cell incubator under 5% CO<sub>2</sub> at 37°C.

**Cell Transfection**

The small interfering RNA of circPRKCI (si-circPRKCI) and its negative control (si-NC) were bought from Guangzhou RiboBio Co., Ltd (Guangzhou, China), and circPRKCI OE and miR-219a-5p mimics were formulated by GenePharma (Shanghai, China). When more than 60% of the cells adhered to the wall, they were transfected using Lipo3000 (Invitrogen, Carlsbad, CA, USA) in line with the instructions of the manufacturer. Finally, the culture of the transfected cells was performed in the incubator under 5% CO<sub>2</sub> at 37°C.

**Quantitative Reverse Transcription-Polymerase Chain Reaction (qRT-PCR)**

TRIzol reagent from Invitrogen (Carlsbad, CA, USA) was utilized to extract the total RNAs from the tissues and cells according to the instructions. Then the total RNAs were subjected to RT into complementary deoxy-ribose nucleic acids (cDNAs) by PrimeScript RT kits (Invitrogen, Carlsbad, CA, USA), and qRT-PCR was implemented using Bio-Rad CFX96 and SYBR Green Premix Ex Taq II from TaKaRa (Dalian, China), with glyceraldehyde-3-phosphate dehydrogenase (GAPDH) and U6 as internal references. The primer sequences were displayed below: CircPRKCI-F: 5'-ATTCAGGGACACCCGTTCTT-3', CircPRKCI-R: 5'-CTCTTCAGAACACTTG-CAGCTT-3'. MiR-219a-5p-F: 5'-TCTACAGTGCACGTGTCTCCAGT-3', MiR-219a-5p-R: 5'-CUCUCAUUUGCUAUUUAUCA-3'. GAPDH-F: 5'-ATGGGGAAGGTGAAGGTCG-3', GAPDH-R: 5'-GGGGTCATTGATGGCAA-CAATA-3'. Calcium/calmodulin dependent protein kinase ID (CAMK1D)-F: 5'-CATAGGACTGGAAGACCGAAGTTTT-3', CAMK1D-R: 5'-CTCGAGTCAGTACAGTTTGTGAGAA-3'. U6-F: 5'-CTCGCTTCGGCAGCACA-3', U6-R: 5'-ACGCTTACGAATTTGCGT-3'.

**Cell Counting Kit-8 (CCK-8) Assay**

After transfection, A549 and H1299 cells were resuspended in a Roswell Park Memorial Institute-1640 (RPMI-1640) medium with FBS, seeded into a ninety-six-well plate at  $2 \times 10^4$  cells/well and further cultured in the incubator. Next, each well of the plate was added with 10  $\mu$ L of CCK-8 reagent provided by Dojindo (Kumamoto, Japan) at 0, 24, 48, 72 and 96 h separately, followed by culture in the incubator for another

1 h. Finally, the optical density (OD) value at 450 nm was measured using a microplate reader, based on which proliferation curves were plotted.

**5-Ethynyl-2'-Deoxyuridine (EdU) Assay**

The capacity of the cells to proliferate was detected via Click-iT EdU imaging kits (Invitrogen, Carlsbad, CA, USA) as per the manufacturer's instructions, and the transfected A549 and H1299 cells were inoculated into the 96-well plate through the EdU method. After 48 h of incubation, the cells in each well were added with 50  $\mu$ M EdU and received incubation again at 37°C under 5% CO<sub>2</sub> for 2 h, followed by fixation with 4% paraformaldehyde. Subsequently, the cells were dyed by 4',6-diamidino-2-phenylindole (DAPI) for 30 min, and the EdU-positive cells were observed under a microscope (Olympus, Tokyo, Japan). Finally, the proliferative ability of the cells was determined based on the ratio of fluorescence positive cells to total cells.

**Transwell Assay**

Transwell chambers with the pore size of 8.0  $\mu$ m (Costar, Corning Incorporated, Corning, NY, USA) were utilized to examine the migratory ability of cells. In short, the cells were resuspended in an FBS-free RPMI-1640 medium after transfection and then seeded into the upper transwell chamber ( $1.0 \times 10^5$  cells/well), while the lower chamber was added with 500  $\mu$ L of Roswell Park Memorial Institute-1640 (RPMI-1640) medium with 10% FBS. Subsequent to incubation in the 5% CO<sub>2</sub> cell incubator at 37°C for 24 h, the cells were immobilized using 4% paraformaldehyde and dyed by 1% crystal violet (Sigma-Aldrich, St. Louis, MO, USA). Finally, the non-transmembrane cells in the upper chamber were gently wiped off using cotton swabs, observed, photographed and counted under the microscope, so as to evaluate the migratory ability of cells.

**Cell Cycle Test**

The transfected A549 and H1299 cells were digested, immobilized in 70% ice-cold ethanol and dyed by propidium iodide (PI) solution with RNase A. Afterwards, a fluorescence-activated cell sorter (FACSVerse, BD, Franklin Lakes, NJ, USA) was utilized to count the dyed cells, and the number of cells in every cycle was assessed using BD FACSuite software.

### Dual-Luciferase Reporter Gene Assay

The sequences in the circPRKCI containing binding sites to miR-219a-5p were inserted into psiCHECK-2 Luciferase reporter vectors (Promega, Madison, WI, USA) to establish circPRKCI-wild type (WT) or circPRKCI-mutant (MUT) Luciferase reporters. Subsequently, A549 and H1299 cells were subjected to transfection with circPRKCI-WT or circPRKCI-MUT and miR-NC or miR-219a-5p mimics. After 48 h, Dual-Luciferase reporter gene assay kits bought from Promega (Madison, WI, USA) were applied to examine the Luciferase activity.

### Statistical Analysis

Statistical analysis was implemented using Statistical Product and Service Solutions (SPSS) 15.0 software (SPSS Inc., Chicago, IL, USA). The data were presented as mean  $\pm$  standard deviation. Intergroup differences were evaluated by Student's *t*-test, and Pearson method was adopted for correlation analysis. The overall survival difference was evaluated by the Kaplan-Meier curves and log rank test.  $p \leq 0.05$  suggested statistical significance. All the assays were separately repeated for 3 times.

### Results

#### CircPRKCI Was Abnormally Highly Expressed in LUAD Tissues

First, qRT-PCR assay was applied to examine the expression level of circPRKCI in 50 cases of LUAD tissues and 50 cases of normal tissues, and it was shown that circPRKCI was expressed at a remarkably higher level in LUAD tissues relative to that in normal tissues (Figure 1A). Meanwhile, the expression level of circPRKCI in tumor tissues of LUAD patients with a tumor diameter  $< 2$  cm and  $\geq 2$  cm was measured *via* qRT-PCR assay. It could be inferred that the LUAD patients with a tumor diameter  $\geq 2$  cm expressed circPRKCI at a higher level in tumor tissues (Figure 1B). Later, the relationship between circPRKCI expression level and tumor stage in patients was analyzed. As shown in Figure 1C, circPRKCI expression level rose up in high-stage tumor tissues in contrast with that in low-stage tumor tissues. Subsequently, the effects of circPRKCI on lymph node metastasis and overall survival rate of LUAD patients were analyzed, and it was found that the highly expressed circPRKCI was more prone to causing the metastasis of lymph nodes (Figure

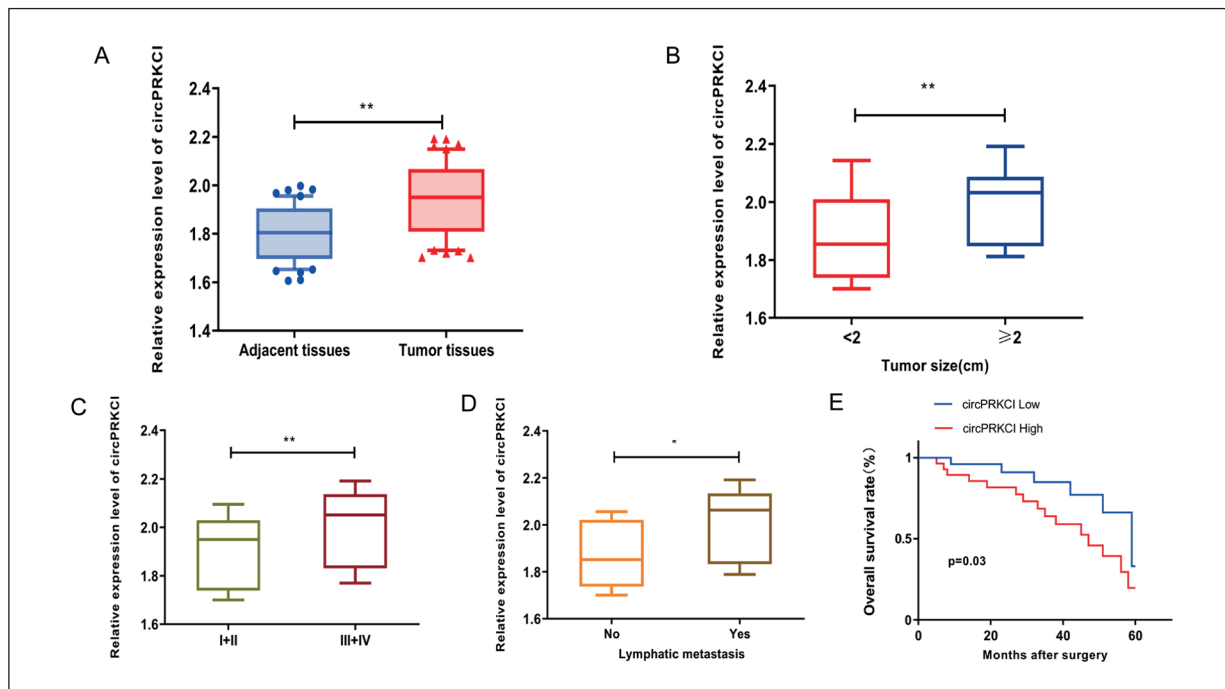


**Figure 1.** CircPRKCI was highly expressed in LUAD. **A**, Relative expression level of circPRKCI in LUAD tissues and normal tissues detected via qRT-PCR assay. **B**, Relative expression level of circPRKCI in different tumor diameters according to analysis. **C**, Relative expression level of circPRKCI in different tumor stages according to analysis. **D**, Relative expression level of circPRKCI in tissues with or without lymph node metastasis according to analysis. **E**, Correlation between circPRKCI expression level and patient's overall survival rate according to analysis. \*\* $p < 0.01$ .

1D), as well as a low survival rate of LUAD patients (Figure 1E). All these results demonstrate that circPRKCI may be related to the poor prognosis of LUAD patients.

### Inhibiting CircPRKCI Repressed LUAD Cells to Migrate and Proliferate as Well as Cell Cycle

To study the influence of circPRKCI on the malignant phenotype of LUAD, circPRKCI expression in normal HBE cells and 4 LUAD cell lines (A549, H1299, H1975 and Calu-3) was de-

termined using qRT-PCR assay first. The findings revealed that circPRKCI expression level rose clearly in LUAD cells in comparison with that in normal HBE cells. Furthermore, the A549 and H1299 cells with apparent expression differences were selected for subsequent experiments (Figure 2A). Second, the expression of circPRKCI in LUAD cells was knocked down by si-circPRKCI, and the interference efficiency was verified by qRT-PCR assay. It was illustrated that the expression level of circPRKCI declined distinctly in cells transfected with

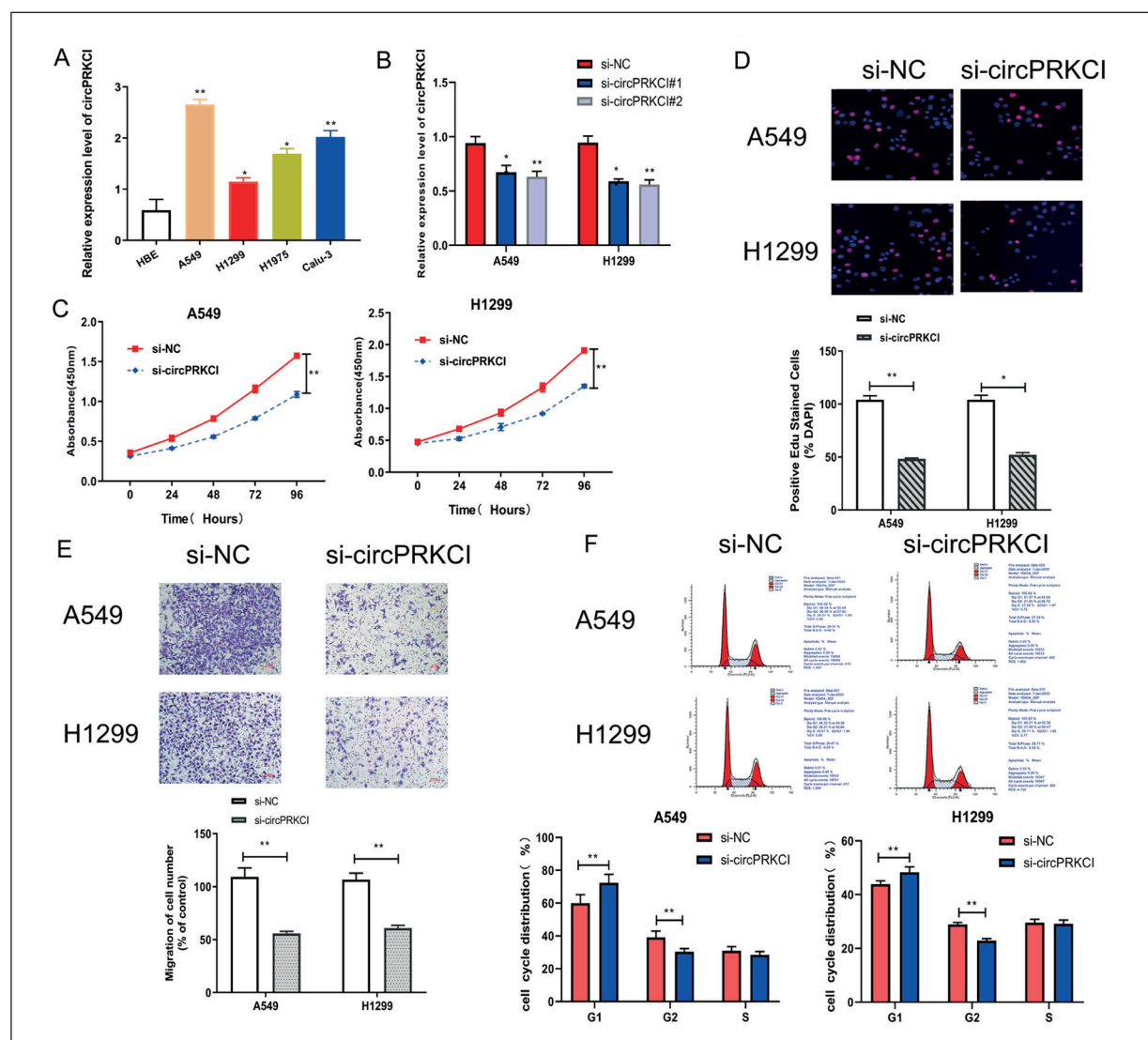


**Figure 2.** Inhibiting circPRKCI could repress proliferation and migration and induce cell cycle arrest. **A**, Expression level of circPRKCI in normal HBE cells and LUAD cell lines measured by qRT-PCR assay. **B**, Expression level of circPRKCI in A549 and H1299 cells transfected with si-NC and si-circPRKCI investigated through qRT-PCR assay. **C**, Effect of circPRKCI knockdown on proliferative ability of A549 and H1299 cells determined by CCK-8 assay. **D**, Proliferative ability of LUAD cells after knocking down circPRKCI examined via EdU assay (magnification: 200 $\times$ ). **E**, Migratory ability of A549 and H1299 cells after knocking down circPRKCI detected through transwell assay (magnification: 200 $\times$ ). **F**, Effect of circPRKCI knockdown on cycle of A549 and H1299 cells indicated using cell cycle test. \* $p < 0.05$ , \*\* $p < 0.01$ .

si-circPRKCI relative to that in cells transfected with si-NC (Figure 2B). Third, the CCK-8 assay was utilized to detect the cell proliferation, and it was denoted that the OD value at 450 nm in A549 and H1299 cells receiving si-circPRKCI transfection was evidently lower than that in cells undergoing si-NC transfection (Figure 2C). In the meantime, the results of EdU assay also revealed that there were fewer EDU-positive A549 and H1299 cells receiving si-circPRKCI transfection than those transfected undergoing si-NC transfection (Figure 2D). Fourth, transwell migration experiment was implemented to examine the migratory ability of cells, and it was discovered that the migratory ability of A549 and H1299 cells transfected with si-circPRKCI was restrained markedly (Figure 2E). Finally, the impact of circPRKCI on LUAD cell cycle was tested using a flow cytometer, and the findings indicated that circPRKCI arrested the cycle of A549 and H1299 cells in the G1 phase (Figure 2F).

### CircPRKCI Could Bind to MiR-219a-5p

For probing the molecular mechanism of circPRKCI in LUAD, the RNAs that might bind to circPRKCI were screened by means of bioinformatics websites, and miR-219a-5p with the highest binding score was selected (Figure 3A). According to the results of Dual-Luciferase reporter gene assay, circPRKCI-WT instead of circPRKCI-MUT was capable of binding to miR-219a-5p (Figure 3B). QRT-PCR was implemented to measure miR-219a-5p expression level in LUAD tissues, and it was unveiled that LUAD tissues exhibited a notably lower expression level of miR-219a-5p than normal tissues (Figure 3C). Next, the Pearson method was adopted to association the relation between circPRKCI and miR-219a-5p, and it was manifested that the relative expression level of miR-219a-5p had an inverse association with that of circPRKCI (Figure 3D). Finally, miR-219a-5p expression level in A549 and H1299 cells undergoing transfection with si-NC or si-circPRKCI

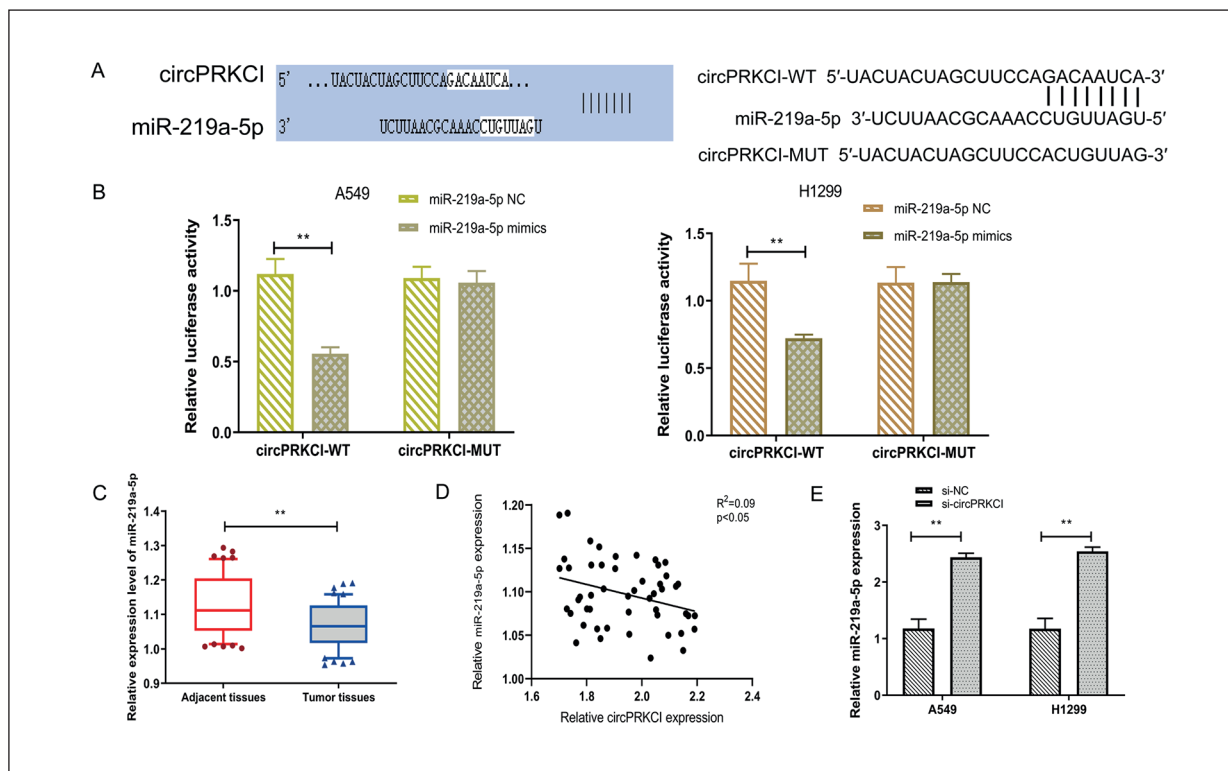


**Figure 3.** CircPRKCI could bind to miR-219a-5p. **A**, MiRNAs with binding sites to the 3'UTR of circPRKCI predicted using bioinformatics websites, and screened miR-219a-5p with a relatively high binding score. **B**, Associative relation between circPRKCI and miR-219a-5p examined via dual-Luciferase reporter gene assay. **C**, Expression level of miR-219a-5p in LUAD tissues detected via qRT-PCR assay. **D**, Correlation between relative expression levels of miR-219a-5p and circPRKCI in LUAD tissues. **E**, Expression level of miR-219a-5p in H1299 and A549 cells transfected with si-NC and si-circPRKCI measured by means of qRT-PCR assay. \*\* $p<0.01$ .

was analyzed by means of qRT-PCR assay. The results demonstrated that it was raised in LUAD cells receiving si-circPRKCI transfection relative to that in cells transfected with si-NC (Figure 3E).

### ***CircPRKCI Regulated LUAD Cells to Proliferate and Migrate as Well as Cell Cycle Via MiR-219a-5p***

For the aim of further exploring the impact of circPRKCI on the malignant phenotype of LUAD through linking to miR-219a-5p, miR-219a-5p inhibitor and si-circPRKCI were transfected into A549 and H1299 cells. Based on the results, circPRKCI was expressed at a lower level in LUAD cells undergoing transfection with si-circPRKCI and miR-219a-5p inhibitor than that in cells receiving miR-219a-5p inhibitor transfection, but at a higher level relative to that in cells receiving si-NC transfection (Figure 4A). Afterwards, the CCK-8 assay results denoted that the OD value at the wavelength of 450 nm was increased in LUAD cells undergoing transfection with si-circPRKCI and miR-219a-5p inhibitor in contrast with that in cells receiving si-NC transfection but decreased in contrast with that in cells undergoing miR-219a-5p inhibitor transfection (Figure 4B). In the meantime, it was revealed in the EdU assay results that there were more EDU-positive LUAD cells undergoing transfection with si-circPRKCI and miR-219a-5p inhibitor than those receiving si-NC transfection, but less than cells undergoing miR-219a-5p inhibitor transfection (Figure 4C). According to Figure 4B & 4C, knocking down miR-219a-5p could partially reverse the inhibition of the proliferative ability of LUAD cells by lowly expressed circPRKCI. After that, the migration of LUAD cells was tested *via* transwell assay. Figure 4D displayed that the number of LUAD cells receiving transfection si-circPRKCI and miR-219a-5p inhibitor was prominently smaller than that of cells transfected with miR-219a-5p inhibitor but larger than that of cells transfected with si-NC. In other words, knocking down miR-219a-5p partially reversed the migratory ability of LUAD cells repressed by lowly expressed circPRKCI. Moreover, the results of cell cycle test also demonstrated that the arrest of LUAD cell cycle in the G1 phase caused by lowly expressed circPRKCI could be partially reversed through the knockdown of miR-219a-5p (Figure 4E).

### ***CAMK1D Was Able to Conjugate With MiR-219a-5p***

The downstream target genes of miR-129a-5p were further screened using bioinformatics websites, and CAMK1D with a high binding score was screened out (Figure 5A). In addition, the associative relation between miR-129a-5p and CAMK1D was determined by means of Dual-Luciferase reporter gene assay. It was shown that miR-129a-5p was capable of binding to CAMK1D-WT rather than CAMK1D-MUT (Figure 5B). The qRT-PCR assay results of CAMK1D expression level in LUAD tissues denoted that CAMK1D exhibited an aberrant high expression in LUAD tissues (Figure 5C). Besides, the association of the expression level of CAMK1D with that of miR-219a-5p or circPRKCI was analyzed by Pearson method, and it was displayed that the relative expression levels of CAMK1D were inversely associated with miR-219a-5p but positively related to circPRKCI (Figure 5D). The above findings elucidate that circPRKCI probably modulates CAMK1D expression by binding to miR-219a-5p in the case of LUAD.

## **Discussion**

Although the morbidity and mortality rates of NSCLC have certain regional characters, the number of deaths from NSCLC is constantly rising in the world<sup>19</sup>. Most LUAD patients have been in the advanced stage when diagnosed, accompanied with distant metastasis at the same time. The therapeutic methods for progressive LUAD include surgery, chemotherapy, radiotherapy, molecular targeted therapy or combination therapy, but the prognosis of LUAD patients remains unsatisfactory owing to the resistance to chemotherapy or radiotherapy, and their 5-year survival rate remains very low (merely 15%)<sup>20,21</sup>. In this research, the results of qRT-PCR assay indicated that circPRKCI exhibited an abnormally high expression in LUAD, so it was conjectured that circPRKCI may act as an oncogene in LUAD and perform vital biological functions through certain molecular mechanisms.

As a kind of endogenous RNAs, circRNAs are formed by skipping or back splicing of exons, with 5'-3' terminals and a lack of polyadenylic acid tails. Nevertheless, rare attention has been paid to their post-transcriptional regulatory functions before discovery<sup>22</sup>. Previous studies

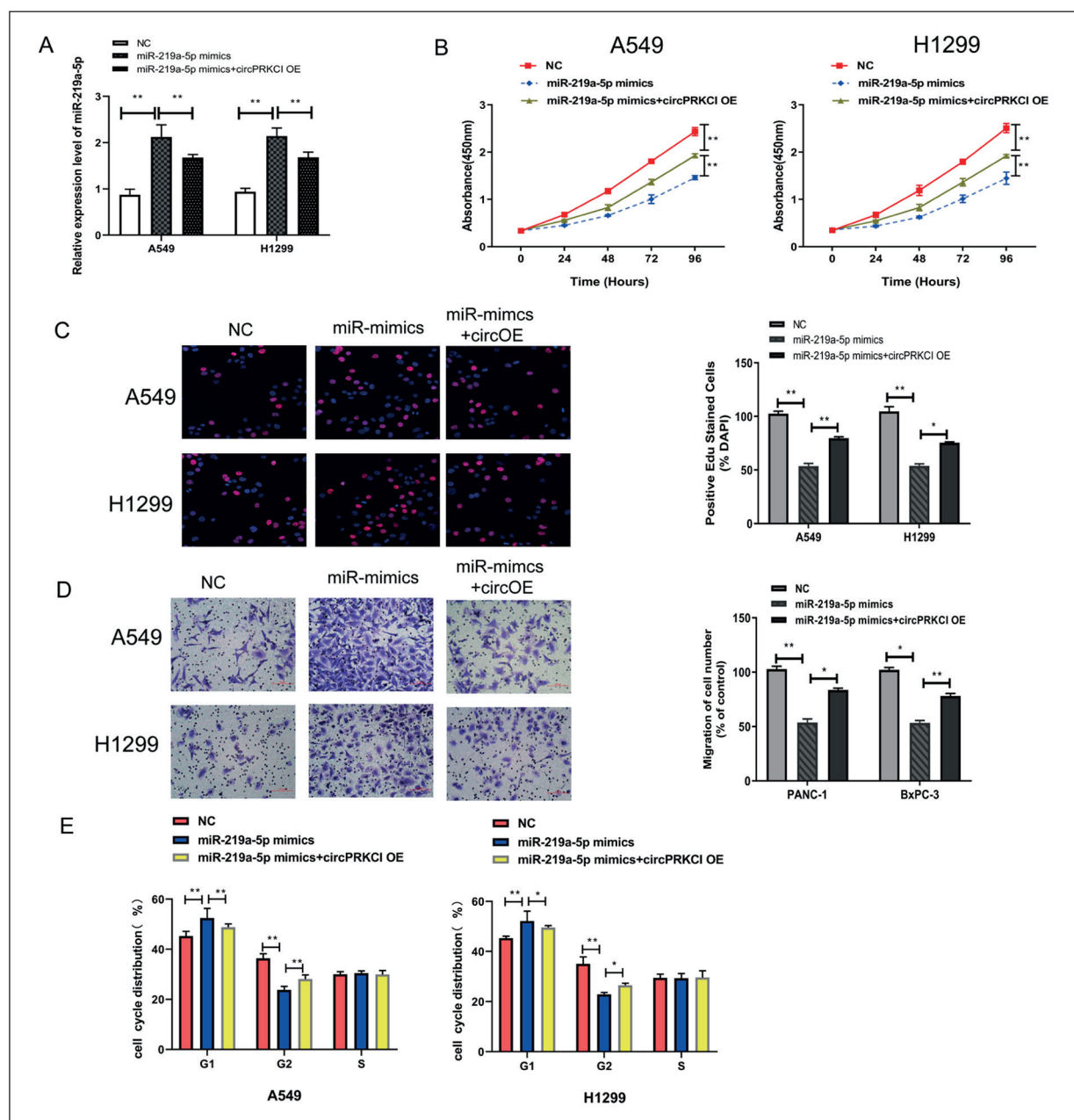


**Figure 4.** Knocking down miR-219a-5p could partially reverse the influence of circPRKCI on the malignant phenotype of LUAD. **A**, Expression level of circPRKCI tested using qRT-PCR assay after co-transfection of A549 and H1299 cells with miR-219a-5p inhibitor and si-circPRKCI. **B**, Effect of co-transfection with miR-219a-5p inhibitor and si-circPRKCI on proliferative ability of A549 and H1299 cells detected via CCK-8 assay. **C**, Effect of co-transfection with miR-219a-5p inhibitor and si-circPRKCI on proliferative ability of A549 and H1299 cells determined by EdU assay (magnification: 200 $\times$ ). **D**, Migratory ability of A549 and H1299 cells after co-transfection with miR-219a-5p inhibitor and si-circPRKCI examined using transwell assay (magnification: 200 $\times$ ). **E**, Effect of co-transfection with miR-219a-5p inhibitor and si-circPRKCI on A549 and H1299 cell cycles detected *via* cell cycle test. \* $p$ <0.05, \*\* $p$ <0.01.

showed that circRNAs usually function as miRNA sponges for miRNA. In recent years, there are increasingly more studies on circPRKCI in human malignancies. Notably, circPRKCI pro-

motes the growth of glioma cells by inhibiting miR-545<sup>23</sup>. CircPRKCI, a competitive endogenous RNA, regulates AKT3 expression through binding to miR-3680-3p in ESCC<sup>24</sup>. Additional-

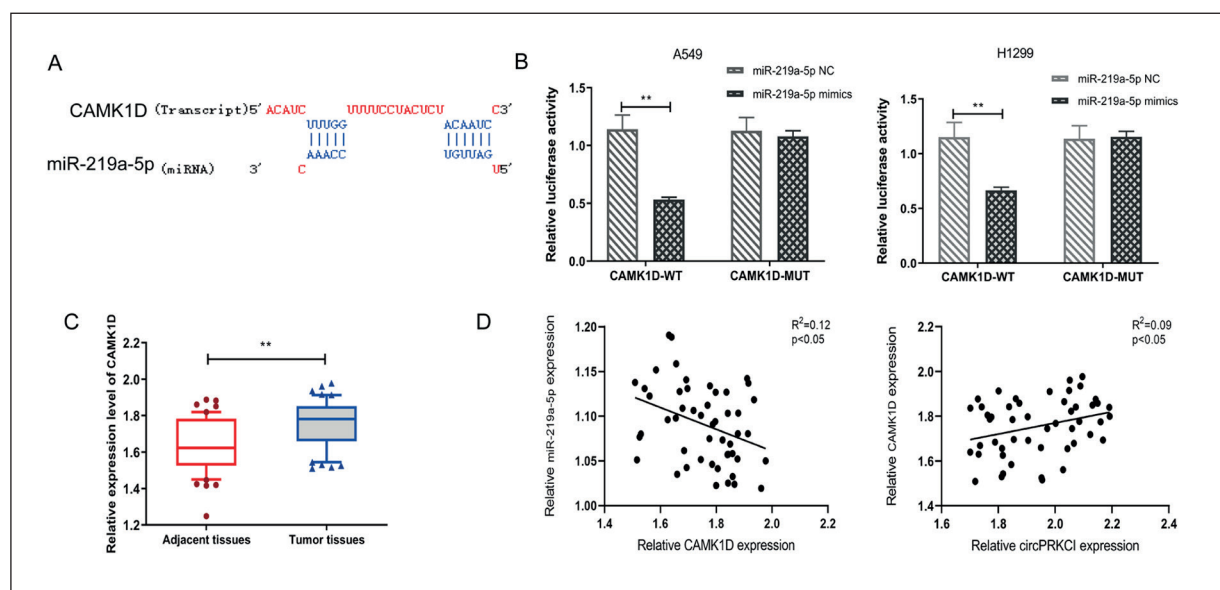


**Figure 5.** CAMK1D could conjugate with miR-219a-5p. **A**, Downstream target genes of miR-219a-5p predicted using bioinformatics websites, and screened CAMK1D with a high binding score. **B**, Associative relation between CAMK1D and miR-219a-5p detected by Dual-Luciferase reporter gene assay. **C**, Expression level of CAMK1D in LUAD tissues measured *via* qRT-PCR assay. **D**, Correlation between relative expression levels of CAMK1D and circPRKCI or miR-219a-5p in LUAD tissues based on correlation analysis.

ly, circPRKCI facilitates gastric cancer cells to proliferate and invade by conjugating with miR-545<sup>25</sup>. The molecular mechanism of circPRKCI in LUAD was investigated preliminarily in this research as the investigation of circPRKCI in LUAD has not been completed, and more studies are necessary.

MiRNAs affect the onset and progression of tumors by modulating the expression of key regulatory factors for tumor proliferation, migration and invasion<sup>26</sup>. MiR-219a-5p exerts an essential effect in human malignant tumors. So, miR-219a-5p impedes the invasion and metastasis of osteosarcoma cells *via* targeting EYA2<sup>27</sup>. MiR-219a-5p targets myocardin-related transcription factor A to repress the migration and EMT of breast cancer cells<sup>28</sup>. Besides, lncRNA SNHG14 stimulates the proliferation and metastasis of ovarian cancer cells through sponging miR-219a-5p<sup>29</sup>. It was found by means of bioinformatics websites in this research that miR-219a-5p possessed binding domains to circPRKCI 3'UTR. Meanwhile, the results of Dual-Luciferase reporter gene assay and qRT-PCR assay indicated that miR-219a-5p could conjugate with circPRKCI, and its expression level was negatively correlated with that of circPRKCI. Based on reverse experiment results, circPRKCI was

able to regulate the malignant phenotype of LUAD *via* binding to miR-219a-5p. MiR-219a-5p intensifies sensitivity of human NSCLC to cisplatin by targeting FGF9<sup>30</sup>, but in-depth exploration should be conducted to perfect the research on miR-219a-5p in the case of LUAD.

CAMK1D belongs to the CaMK-regulated serine/threonine protein kinase family (CaMK family)<sup>31</sup>. The CaMK family is primarily researched in neurons and lymphocytes, which plays roles in different cellular processes. CAMK1D shares an amino acid homology of 77% with CAMKI, which was first cloned from neutrophils<sup>32</sup>. Previously, CAMK1D was found to have important biological effects on breast cancer<sup>33</sup> and lung cancer<sup>34</sup>. The novelty of this study was that our present research revealed that CAMK1D was a potential target gene of miR-219a-5p, and they could bind to each other according to the Dual-Luciferase reporter gene assay. Moreover, the Pearson analysis denoted that CAMK1D was negatively correlated with miR-219a-5p and positively associated with circPRKCI in terms of the relative expression level, manifesting that circPRKCI may modulate CAMK1D expression through linking to miR-219a-5p. The aforementioned findings may provide novel targets for treating LUAD.

## Conclusions

It was discovered in this research that circPRKCI is prominently highly expressed LUAD tissues and cell lines, and the high circPRKCI expression probably results in unfavorable prognosis of LUAD patients. CircPRKCI regulates the proliferation, migration and cell cycle of LUAD through the miR-219a-5p/CAMK1D axis, which probably becomes a new target for treating LUAD.

## Conflict of Interest

The Authors declare that they have no conflict of interests.

## References

- Siegel RL, Miller KD, Jemal A. Cancer statistics, 2016. *CA Cancer J Clin* 2016; 66: 7-30.
- Huang JY, Cui SY, Chen YT, Song HZ, Huang GC, Feng B, Sun M, De W, Wang R, Chen LB. MicroRNA-650 was a prognostic factor in human lung adenocarcinoma and confers the docetaxel chemoresistance of lung adenocarcinoma cells via regulating Bcl-2/Bax expression. *PLoS One* 2013; 8: e72615.
- Gettinger S, Lynch T. A decade of advances in treatment for advanced non-small cell lung cancer. *Clin Chest Med* 2011; 32: 839-851.
- Vora N, Reckamp KL. Non-small cell lung cancer in the elderly: defining treatment options. *Semin Oncol* 2008; 35: 590-596.
- Kristensen LS, Hansen TB, Venø MT, Kjems J. Circular RNAs in cancer: opportunities and challenges in the field. *Oncogene* 2018; 37: 555-565.
- Memczak S, Papavasileiou P, Peters O, Rajewsky N. Identification and characterization of circular RNAs as a new class of putative biomarkers in human blood. *PLoS One* 2015; 10: e141214.
- Shang Q, Yang Z, Jia R, Ge S. The novel roles of circRNAs in human cancer. *Mol Cancer* 2019; 18: 6.
- Salzman J. Circular RNA expression: its potential regulation and function. *Trends Genet* 2016; 32: 309-316.
- Bian L, Zhi X, Ma L, Zhang J, Chen P, Sun S, Li J, Sun Y, Qin J. Hsa\_circRNA\_103809 regulated the cell proliferation and migration in colorectal cancer via miR-532-3p / FOXO4 axis. *Biochem Biophys Res Commun* 2018; 505: 346-352.
- Chen L, Zhang S, Wu J, Cui J, Zhong L, Zeng L, Ge S. circRNA\_100290 plays a role in oral cancer by functioning as a sponge of the miR-29 family. *Oncogene* 2017; 36: 4551-4561.
- Chen D, Ma W, Ke Z, Xie F. CircRNA hsa\_circ\_100395 regulates miR-1228/TCF21 pathway to inhibit lung cancer progression. *Cell Cycle* 2018; 17: 2080-2090.
- Ke XS, Liu CM, Liu DP, Liang CC. MicroRNAs: key participants in gene regulatory networks. *Curr Opin Chem Biol* 2003; 7: 516-523.
- Iorio MV, Croce CM. MicroRNA dysregulation in cancer: diagnostics, monitoring and therapeutics. A comprehensive review. *EMBO Mol Med* 2012; 4: 143-159.
- Mendell JT, Olson EN. MicroRNAs in stress signaling and human disease. *Cell* 2012; 148: 1172-1187.
- Yang L, Li C, Liang F, Fan Y, Zhang S. MiRNA-155 promotes proliferation by targeting caudal-type homeobox 1 (CDX1) in glioma cells. *Biomed Pharmacother* 2017; 95: 1759-1764.
- He J, Tang Y, Tian Y. MicroRNA214 promotes proliferation and inhibits apoptosis via targeting Bax in nasopharyngeal carcinoma cells. *Mol Med Rep* 2015; 12: 6286-6292.
- Wang L, Mo H, Jiang Y, Wang Y, Sun L, Yao B, Chen T, Liu R, Li Q, Liu Q, Yin G. MicroRNA-519c-3p promotes tumor growth and metastasis of hepatocellular carcinoma by targeting BTG3. *Biomed Pharmacother* 2019; 118: 109267.
- Qiu M, Xia W, Chen R, Wang S, Xu Y, Ma Z, Xu W, Zhang E, Wang J, Fang T, Hu J, Dong G, Yin R, Wang J, Xu L. The circular RNA circPRKCI promotes tumor growth in lung adenocarcinoma. *Cancer Res* 2018; 78: 2839-2851.
- Dela CC, Tanoue LT, Matthay RA. Lung cancer: epidemiology, etiology, and prevention. *Clin Chest Med* 2011; 32: 605-644.
- Gettinger S, Lynch T. A decade of advances in treatment for advanced non-small cell lung cancer. *Clin Chest Med* 2011; 32: 839-851.
- Sun Y, Fang R, Li C, Li L, Li F, Ye X, Chen H. Hsa-mir-182 suppresses lung tumorigenesis through down regulation of RGS17 expression in vitro. *Biochem Biophys Res Commun* 2010; 396: 501-507.
- Memczak S, Jens M, Elefsinioti A, Torti F, Krueger J, Rybak A, Maier L, Mackowiak SD, Gregersen LH, Munschauer M, Loewer A, Ziebold U, Landthaler M, Kocks C, le Noble F, Rajewsky N. Circular RNAs are a large class of animal RNAs with regulatory potency. *Nature* 2013; 495: 333-338.
- Zhang X, Yang H, Zhao L, Li G, Duan Y. Circular RNA PRKCI promotes glioma cell progression by inhibiting microRNA-545. *Cell Death Dis* 2019; 10: 616.
- Shi N, Shan B, Gu B, Song Y, Chu H, Qian L. Circular RNA circ-PRKCI functions as a competitive endogenous RNA to regulate AKT3 expression by sponging miR-3680-3p in esophageal squamous cell carcinoma. *J Cell Biochem* 2019; 120: 10021-10030.
- Wu L, Li Y, Xu XM, Zhu X. Circular RNA circ-PRKCI promotes cell proliferation and invasion by binding to microRNA-545 in gastric cancer. *Eur Rev Med Pharmacol Sci* 2019; 23: 9418-9426.

- 26) Wang Y, Chen T, Huang H, Jiang Y, Yang L, Lin Z, He H, Liu T, Wu B, Chen J, Kamp DW, Liu G. miR-363-3p inhibits tumor growth by targeting PCNA in lung adenocarcinoma. *Oncotarget* 2017; 8: 20133-20144.
- 27) Zhu X, Chen L, Lin J. miR-219a-5p represses migration and invasion of osteosarcoma cells via targeting EYA2. *Artif Cells Nanomed Biotechnol* 2018; 46: S1004-S1010.
- 28) Zhuang C, Yuan Y, Song T, Wang H, Huang L, Luo X, He H, Huo L, Zhou H, Wang N, Zhang T. miR-219a-5p inhibits breast cancer cell migration and epithelial-mesenchymal transition by targeting myocardin-related transcription factor A. *Acta Biochim Biophys Sin (Shanghai)* 2017; 49: 1112-1121.
- 29) Li L, Zhang R, Li SJ. Long noncoding RNA SNHG14 promotes ovarian cancer cell proliferation and metastasis via sponging miR-219a-5p. *Eur Rev Med Pharmacol Sci* 2019; 23: 4136-4142.
- 30) Rao C, Miao X, Zhao G, Zhang C, Shen H, Dong C, Yang M. MiR-219a-5p enhances cisplatin sensitivity of human non-small cell lung cancer by targeting FGF9. *Biomed Pharmacother* 2019; 114: 108662.
- 31) Hook SS, Means AR. Ca(2+)/CaM-dependent kinases: from activation to function. *Annu Rev Pharmacol Toxicol* 2001; 41: 471-505.
- 32) Verploegen S, Lammers JW, Koenderman L, Coffey PJ. Identification and characterization of CK-LiK, a novel granulocyte Ca(++)/calmodulin-dependent kinase. *Blood* 2000; 96: 3215-3223.
- 33) Bergamaschi A, Kim YH, Kwei KA, La Choi Y, Bocanegra M, Langerod A, Han W, Noh DY, Huntsman DG, Jeffrey SS, Borresen-Dale AL, Pollack JR. CAMK1D amplification implicated in epithelial-mesenchymal transition in basal-like breast cancer. *Mol Oncol* 2008; 2: 327-339.
- 34) Lawson J, Dickman C, MacLellan S, Towle R, Jabalee J, Lam S, Garnis C. Selective secretion of microRNAs from lung cancer cells via extracellular vesicles promotes CAMK1D-mediated tube formation in endothelial cells. *Oncotarget* 2017; 8: 83913-83924.